

Freezeout conditions in proton-proton collisions at the top RHIC and LHC energies

Sabita Das,^{1,2,*} Debadeepti Mishra,^{2,†} Sandeep Chatterjee,^{2,‡} and Bedangadas Mohanty^{2,§}

¹*Institute of Particle Physics and Key Laboratory of Quark & Lepton Physics (MOE) ,
Central China Normal University, Wuhan-430079, China*

²*School of Physical Sciences,
National Institute of Science Education and Research, HBNI, Jatni-752050, India*

Abstract

The freezeout conditions in proton-proton collisions at $\sqrt{s_{\text{NN}}} = 200, 900$ and 7000 GeV have been extracted by fits to the mean hadron yields at mid-rapidity within the framework of the statistical model of an ideal gas of hadrons and resonances in the grand canonical ensemble. The variation of the extracted freezeout thermal parameters and the goodness of the fits with $\sqrt{s_{\text{NN}}}$ are discussed. We find the extracted temperature and baryon chemical potential of the freezeout surface to be similar in p+p and heavy ion collisions. On the other hand, the thermal behaviour of the strange hadrons is qualitatively different in p+p as compared to A+A. We find an additional parameter accounting for non-equilibrium strangeness production is essential for describing the p+p data. This is in contrast to A+A where the non-equilibrium framework could be successfully replaced by a sequential and complete equilibrium model with an early freezeout of the strange hadrons.

* sabita@rcf.rhic.bnl.gov

† debadeepti.m@niser.ac.in

‡ sandeepc@niser.ac.in

§ bedanga@niser.ac.in

I. INTRODUCTION

The statistical model of non-interacting gas of hadrons and resonances at some volume V , temperature T and conserved charge chemical potentials μ_B , μ_Q and μ_S corresponding to the three conserved charges of QCD, namely baryon number B , electric charge Q and strangeness S have been remarkably successful in providing a good qualitative description of the mean hadron yields in heavy ion collision experiments across a wide range of beam energies from AGS to LHC [1–3]. This could possibly indicate a hadronic medium in thermal equilibrium prior to freezeout. However, the extracted thermal parameters indicate that the freezeout surface lies very close to the hadronization surface [4, 5]. This has led to the suggestion that the hadrons are directly born into equilibrium from the quark gluon plasma (QGP) phase instead of there being a microscopic collision mechanism for equilibration [6]. A microscopic collision picture has been suggested by invoking contribution from Hagedorn resonances with exponential mass spectrum [7]. Recently, in yet another approach based on Unruh radiation, an universal freezeout temperature was suggested for systems starting from e+e, p+p to heavy ions [8]. Thus, in spite of the enormous phenomenological success of the thermal models, the microscopic understanding of such fast thermal equilibration is still an open question.

One crucial ingredient in the application of thermal models is the choice of the ensemble to treat the conserved charges. Ideally, conserved charges in an open system should be treated within a grand canonical ensemble (GCE) while those in a closed system should be treated canonically. Thus, 4π data should be treated canonically while for mid-rapidity measurements that represent an open system, grand canonical ensembles should be applicable. However, it is not so straightforward in the case of particle production in relativistic collisions. It is believed that even if the criteria for applicability of GCE, $VT^3 > 1$ holds true for the bulk of the produced particles, canonical suppression might still be required when the number of carriers of a specific conserved charge are few [20]. For this reason, strangeness has been treated canonically in p+p collisions owing to the small system size for the $\sqrt{s_{NN}} = 200$ GeV mid-rapidity data at RHIC [20].

It is interesting to test the framework of thermal models in small systems [17, 18]. Previously, thermal models have been used to describe particle yields in small systems with a fair degree of success [17, 19–22]. It is a commonly accepted notion that in small systems the formation of a thermally equilibrated fireball through multiple scattering of its constituents is less likely than in

A+A collisions. However, it has been demonstrated through explicit application of thermal models that the quality of description of the data is similar for different system sizes [23].

In this paper, we will apply the thermal model on mid-rapidity data in p+p collisions at $\sqrt{s_{\text{NN}}} = 200$ (RHIC), 900 (LHC) and 7000 (LHC) GeV. We find the mid-rapidity data is described by the GCE at all the above $\sqrt{s_{\text{NN}}}$. A comparative study of two different schemes of treating the strange hadrons in p+p collisions - either having a strangeness correlation volume different from the fireball volume or using a strangeness undersaturation factor γ_S - yielded similar goodness of fits for both the schemes [17]. We have kept the strangeness conservation volume equal to the fireball volume, allowing non-equilibrium strangeness production only through the departure from unity of γ_S . At the LHC energies we have fixed the chemical potentials to zero.

II. THERMAL MODEL

In a single chemical freezeout scheme (1CFO) all the hadrons freezeout from the same surface characterised by a single $(V, T, \mu_B, \mu_Q, \mu_S)$. The particle multiplicities become:

$$N_i = \frac{g_i V}{2\pi^2} \sum_{k=1}^{\infty} (\pm 1)^{k+1} \frac{m_i^2 T}{k} K_2 \left(\frac{km_i}{T} \right) \exp(\beta k \mu_i) \gamma_S^{k|S_i|}, \quad (1)$$

where V is the fireball volume, g_i is the degeneracy, m_i is the particle mass, and K_2 is second order Bessel function. $\beta = \frac{1}{T}$, where T is the chemical freezeout temperature. The plus sign is for bosons and the minus sign is for fermions. The hadron chemical potential μ_i in case of complete chemical equilibrium can be written down in terms of μ_B , μ_Q and μ_S as follows

$$\mu_i = B_i \mu_B + Q_i \mu_Q + S_i \mu_S \quad (2)$$

where B_i , Q_i and S_i are the baryon number, charge and strangeness of the i th hadron. It is a standard practice to extract μ_S and μ_Q from the following constraints

$$\text{Net}S = 0 \quad (3)$$

$$\text{Net}B/\text{Net}Q = 1 \quad (4)$$

Eq. 4 is valid only for p+p collisions. In A+A collisions, the unity in the RHS of Eq. 4 should be replaced by ~ 2.5 . The remaining parameters (V, T, μ_B) are extracted from fits to hadron yields.

The total yield $N_i^{\text{tot.}}$ of the i th hadron include primordial yields (produced directly in the reaction) and secondary yields which are the feed-down from the decays of heavier resonances

$$N_i^{\text{tot.}} = N_i^{\text{prim}} + \sum_{\text{states } j} N_j^{\text{prim}} \text{B.R. } (j \rightarrow i), \quad (5)$$

where N_i^{prim} is primordial multiplicity of species i and B.R. ($j \rightarrow i$) is the branching ratio of j to i through all possible channels. We have used the THERMUS code [24] which is available publicly for the 1CFO analysis.

As seen in Eq. 1, there is one more parameter, γ_S which is also treated as a free parameter and extracted from fits to data. It accounts for possible chemical nonequilibrium of strangeness in the fireball. In a complete equilibrium scenario, $\gamma_S = 1$.

III. DATA SETS

We have used the p+p collision mid-rapidity data sets at RHIC with $\sqrt{s_{\text{NN}}} = 200$ GeV [30–32] and at LHC with $\sqrt{s_{\text{NN}}} = 900$ GeV [33, 34] and 7 TeV [35–37]. The π^\pm and Λ are feed-down corrected from weak decays whereas (anti)protons at RHIC are inclusive. The data sets from LHC have π^\pm , p, \bar{p} and Λ that are feed-down corrected from weak decays. The details about the data sets used in this study are given in Table I.

IV. RESULTS

In Fig. 1 we have plotted the fitted freezeout parameters obtained in GCE in 1CFO. Previously, the RHIC $\sqrt{s_{\text{NN}}} = 200$ GeV p+p mid-rapidity data (excluding ϕ) has been fitted in the strangeness canonical ensemble [20]. However, we find here that the GCE provides reasonable description with $\chi^2/ndf \sim 1 - 2$ even when including ϕ . The thermal model results for the mid-rapidity LHC data at $\sqrt{s_{\text{NN}}} = 900$ and 7000 GeV are new. The χ^2/ndf is around 2 – 3 which has marginally increased from the top RHIC energy.

The value of γ_S monotonically rises from 0.6 to 0.8 between RHIC and LHC energies. The freezeout T on the other hand monotonically decreases from 160 MeV at $\sqrt{s_{\text{NN}}} = 200$ GeV to ~ 150 MeV at 7 TeV. The fireball radius rises from ~ 1.3 fm at $\sqrt{s_{\text{NN}}} = 200$ GeV to ~ 1.7 fm at $\sqrt{s_{\text{NN}}} = 7$ TeV. μ_B is relatively flat and hovers around zero.

$\sqrt{s_{\text{NN}}}$ (GeV)	Expt.	System	Particle yields (dN/dy)	Antiparticle yields (dN/dy)	Ref.
200	STAR	p+p	$\pi^+ : 1.44 \pm 0.11$	$\pi^- : 1.42 \pm 0.11$	[30]
			$K^+ : 0.150 \pm 0.013$	$K^- : 0.145 \pm 0.013$	[30]
			$p : 0.138 \pm 0.012$	$\bar{p} : 0.113 \pm 0.010$	[30]
			$\Lambda : 0.0385 \pm 0.0036$	$\bar{\Lambda} : 0.0351 \pm 0.0033$	[31]
			$\Xi^- : 0.0026 \pm 0.0009$	$\bar{\Xi}^+ : 0.0029 \pm 0.001$	[31]
			$K_S^0 : 0.134 \pm 0.011$		[31]
			$\Omega + \bar{\Omega} : 0.00034 \pm 0.00019$		[31]
$\phi : 0.018 \pm 0.003$		[32]			
900	ALICE	p+p	$\pi^+ : 1.493 \pm 0.0741$	$\pi^- : 1.485 \pm 0.0741$	[33]
			$K^+ : 0.183 \pm 0.0155$	$K^- : 0.182 \pm 0.0155$	[33]
			$p : 0.083 \pm 0.0063$	$\bar{p} : 0.079 \pm 0.0063$	[33]
			$\Lambda : 0.048 \pm 0.0041$	$\bar{\Lambda} : 0.047 \pm 0.0054$	[34]
			$\Xi^- + \bar{\Xi}^+ : 0.0101 \pm 0.0022$		[34]
			$K_S^0 : 0.184 \pm 0.0063$		[34]
			$\phi : 0.021 \pm 0.005$		[34]
7000	ALICE	p+p	$\pi^+ : 2.26 \pm 0.1$	$\pi^- : 2.23 \pm 0.1$	[35]
			$K^+ : 0.286 \pm 0.016$	$K^- : 0.286 \pm 0.016$	[35]
			$p : 0.124 \pm 0.009$	$\bar{p} : 0.123 \pm 0.01$	[35]
			$\Xi^- : 0.008 \pm 0.000608$	$\bar{\Xi}^+ : 0.0078 \pm 0.000608$	[36]
			$\Omega : 0.00067 \pm 0.000085$	$\bar{\Omega} : 0.00068 \pm 0.000085$	[36]
			$\phi : 0.032 \pm 0.004$		[37]

TABLE I. Details of the data sets used for fit with references.

200	162.2 ± 3.6	14.4 ± 8.5	0.54 ± 0.03	1.3 ± 0.08	16.3	1.8
900	155.4 ± 2.4	0.0 (Fixed)	0.73 ± 0.03	1.42 ± 0.06	27.0	2.7
7000	152.9 ± 2.0	0.0 (Fixed)	0.75 ± 0.02	1.69 ± 0.05	22.6	2.8

TABLE II. The chemical freezeout parameters extracted in 1CFO scheme in GCE at $\sqrt{s_{\text{NN}}} = 200, 900$ and 7000 GeV.

Earlier, we had noted that the χ^2/ndf marginally rises from the top RHIC to LHC energies. A rise in the χ^2/ndf do not necessarily mean a worsening of the thermal model fits. It could also occur due to more precise measurements. This could be verified by comparing the deviation between model

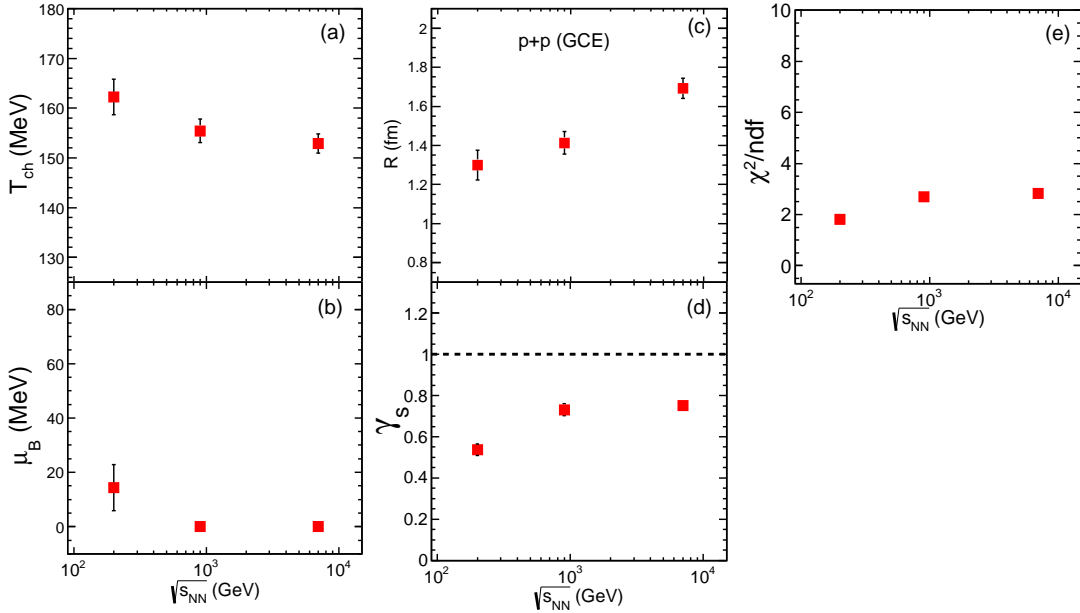


FIG. 1. (Color online) Freezeout parameters T_{ch} , μ_B , γ_S , R and χ^2/ndf obtained from a statistical model fit [24] using mid-rapidity particle yields.

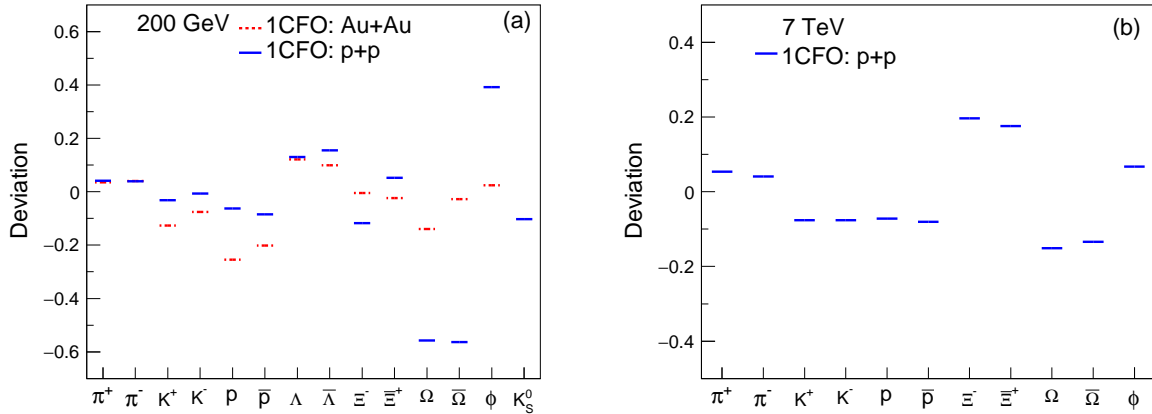


FIG. 2. (Color online) Left: The deviation between model and data for each species in 1CFO at $\sqrt{s_{NN}} = 200$ GeV compared between p+p and heavy ions. Right: The deviation between model and data in 1CFO at $\sqrt{s_{NN}} = 7$ TeV.

and data defined as

$$\text{deviation} = \frac{\text{data} - \text{model}}{\text{data}} \quad (6)$$

Figs. 2 (a) and 2 (b) show the deviation for $\sqrt{s_{NN}} = 200$ and 7000 GeV respectively. At 7000 GeV,

the deviation between data and model for all the hadron species lie within 20%. Even at 200 GeV, we find that except for Ω and ϕ , the deviation for the rest of the hadrons are all within 20%. This shows clearly that the rise in χ^2/ndf from RHIC to LHC is due to more precision measurements at the LHC. Further, in Fig. 2 (a) we have also compared the deviation for each species between p+p and HICs for $\sqrt{s_{NN}} = 200$ GeV. We find that the hadrons with multiple valence strange quarks like ϕ , Ξ and Ω show higher deviation in p+p case compared to HIC.

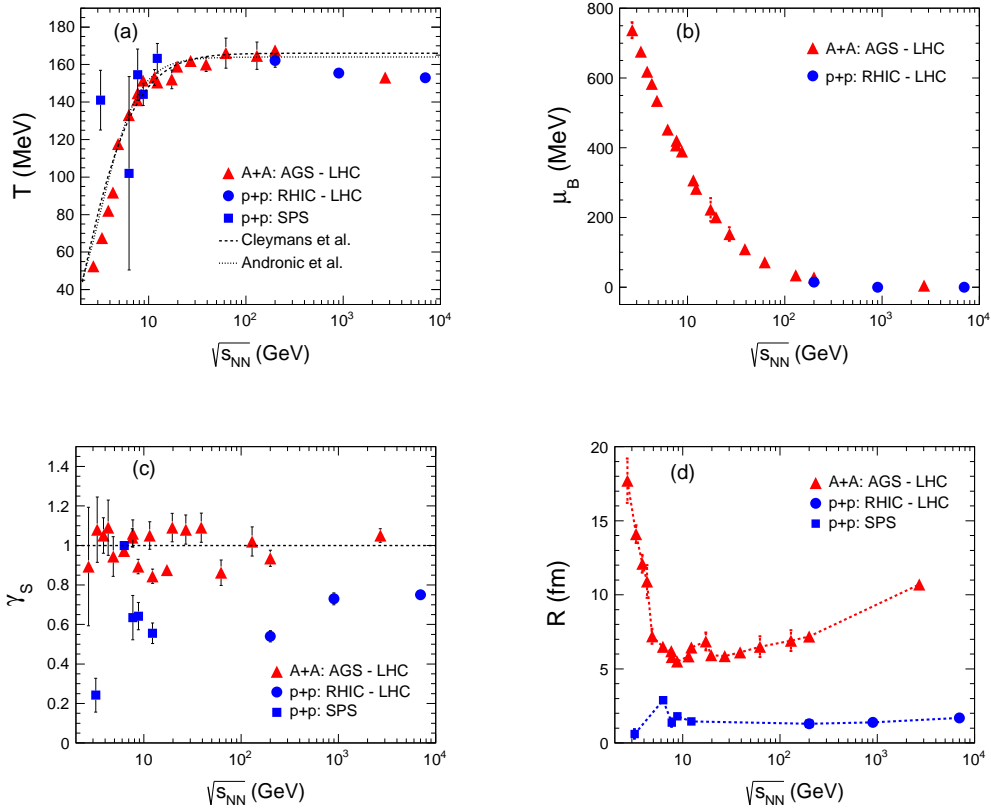


FIG. 3. (Color online) A compilation of T (a), μ_B (b), γ_S (c) and R (d) vs $\sqrt{s_{NN}}$ in p+p collisions shown in blue squares at SPS energies taken from Ref. [22] and blue circles for RHIC and LHC energies which are the results of this paper. The results for A+A are shown in red triangles for comparison [3]. The T vs $\sqrt{s_{NN}}$ parametrizations shown by dashed lines are from Refs. [38] and [39].

Finally, we have compared in Fig. 3 the freezeout parameters T , μ_B , γ_S and R extracted in HICs with that of p+p in 1CFO. At lower $\sqrt{s_{NN}}$, the p+p freezeout T is higher than in A+A as was recently reported [22]. However at higher beam energies ($\sqrt{s_{NN}} > 200$ GeV), the T extracted in p+p

is in agreement to that of HIC. As we go from RHIC to LHC energies, both p+p as well as A+A collisions show a decrease of the freezeout temperature by about 10 MeV. μ_B extracted from p+p is similar to that obtained from A+A. γ_S and R are quite different in the two systems. Between the top SPS and LHC energies, while the R in A+A doubles, the corresponding rise in p+p is only about 20%. In this entire range, the radius in p+p is almost 5 – 10 times smaller compared to A+A. In A+A collisions, γ_S is consistent with unity while in p+p it is around 0.2 at SPS and then steadily rises before saturating around 0.8 at the LHC. This indicates significant strangeness suppression in p+p as compared to heavy ion even at the LHC energies. It will be interesting to see whether at even higher beam energies we produce strangeness in complete equilibrium or not. In this regard we note from Fig. 2 that in p+p there is large deviation between data and model as compared to heavy ion for hadrons with multiple strange valence quarks.

The recent data from Pb+Pb collisions at $\sqrt{s_{NN}} = 2.76$ TeV have renewed the interest in thermal models as the standard 1CFO freezeout scheme failed to explain the data satisfactorily, with a notable disparity between model and experiment in the proton to pion ratio, commonly known as the proton anomaly [9, 10]. Several alternative freezeout schemes have been proposed to address the above issue [11–14]. One of them is the two freezeout scheme (2CFO) where those hadrons with non-zero strangeness content are allowed to freezeout at a different surface as compared to those with zero strangeness [13, 14]. The 2CFO scheme has successfully described the proton anomaly [13] and transverse momentum spectra [15] at LHC, the $\frac{{}^3H}{{}^3He}$ ratio at $\sqrt{s_{NN}} = 200$ GeV and $\frac{\bar{\Lambda}}{p}$ at lower beam energies which can not be described by the 1CFO scheme [3, 16]. We have checked the above p+p data in the 2CFO scheme as well. However, unlike in HICs where the 2CFO scheme provides a much better description of the hadron yields than 1CFO [13], here in p+p collisions we find the χ^2/ndf is similar and one does not gain much by introducing two additional parameters in 2CFO compared to γ_S augmented 1CFO. Thus in p+p collisions, the 1CFO scheme with the additional strangeness suppression factor γ_S seems to be a better scheme than the complete chemical equilibrium but sequential freezeout scheme of 2CFO. The primary motivation for a 2CFO scheme in A+A collision is the expected flavor hierarchy in hadron-hadron cross-sections which result in different flavored hadrons freezing out at different times. However, in p+p collisions hadronic interactions are much reduced and the quick expansion results in a rapid freezeout leaving little room for sequential freezeout to occur.

V. SUMMARY

The freezeout conditions for p+p collisions were extracted from the data on hadron yields at mid-rapidity for $\sqrt{s_{NN}} = 200, 900$ and 7000 GeV. Previous analyses have mostly focussed on a canonical treatment of strangeness in p+p collisions irrespective of the detector acceptance. We performed the analysis in the grand canonical ensemble as it is expected to describe the mid-rapidity system which behaves like an open system.

At these top beam energies, while the extracted temperature and baryon chemical potential is in agreement with those from heavy ion collisions, the strangeness suppression factor comes out to be ~ 0.8 in p+p. Thus the main difference arises in the freezeout condition for the strange hadrons. In A+A collisions, a complete thermal and chemical equilibrium scheme with early freezeout for strangeness provides a good description of the data. However, here in p+p collisions we found that a single freezeout scheme extended by a non-equilibrium factor for strangeness production provides the best description of the data amongst the different ensemble and freezeout schemes. We find a strong strangeness suppression across all the beam energies - about 20% suppression is found even at the highest LHC energies. The expected shorter lifetime of the fireball in case of p+p collisions could be a reason behind such difference in the freezeout behaviour of the strange hadrons.

VI. ACKNOWLEDGEMENT

We acknowledge Jurgen Schucraft for his helpful comments on the manuscript. SD thanks Jean Cleymans for helpful discussions and the MoST of China 973-Project No. 2015CB856901 and XIIth plan project no. 12-R&D-NIS-5.11-0300 of Govt. of India for support. DM acknowledges the support from DAE and DST/SERB project of Govt. of India. SC thanks XIIth plan project no. 12-R&D-NIS-5.11-0300 of Govt. of India for support. BM acknowledges support from DST SwarnaJayanti and DAE-SRC projects.

-
- [1] F. Becattini *et al.*, Phys. Rev. **C64** 024901 (2001).
 - [2] A. Andronic, P. Braun-Munzinger and J. Stachel, Nucl. Phys. **A772** 167-199 (2006).
 - [3] S. Chatterjee *et al.*, Adv. in High Eng. Phys., **2015**, 349013 (2015).

- [4] O. Kaczmarek *et al.*, Phys. Rev. **D83** 014504 (2011).
- [5] G. Endrodi *et. al.*, JHEP **1104** 001 (2011).
- [6] R. Stock, Phys. Lett. **B456** 277-282 (1999).
- [7] J. Noronha-Hostler *et. al.* Phys. Rev. Lett. **100**, 252301 (2008).
- [8] P. Castorina, D. Kharzeev and H. Satz, Eur. Phys. J. **C52**, 187-201 (2007).
- [9] M. Rybczynski, W. Florkowski and W. Broniowski, Phys. Rev. **C85** 054907 (2012).
- [10] J. Stachel *et al.*, J. Phys. Conf. Ser. **509**, 012019 (2014).
- [11] J. Steinheimer, J. Aichelin and M. Bleicher, Phys. Rev. Lett. **110** 042501 (2013).
- [12] M. Petrñ, J. Letessier, V. Petrek and J. Rafelski, Phys. Rev. **C88** 034907 (2013).
- [13] S. Chatterjee, R. Godbole, and S. Gupta, Phys. Lett. **B727**, 554 (2013).
- [14] K. A. Bugaev *et. al.*, Europhys. Lett. **104** 22002 (2013).
- [15] S. Chatterjee, B. Mohanty and R. Singh, Phys. Rev. **C92**, 024917 (2015).
- [16] S. Chatterjee and B. Mohanty, Phys. Rev. **C90**, 034908 (2014).
- [17] I. Kraus *et al.* Phys. Rev. **C76**, 064903 (2007).
- [18] J. Cleymans *et. al.*, arXiv: 1603.09553.
- [19] F. Becattini, U. Heinz, Z. Phys. **C76**, 269 (1997).
- [20] I. Kraus *et al.* Phys. Rev. **C79**, 014901 (2009).
- [21] I. Kraus *et al.* Phys. Rev. **C81**, 024903 (2010).
- [22] V. Vovchenko, V.V. Begun and M.I. Gorenstein, arXiv:1512.08025.
- [23] F. Becattini, P. Castorina, A. Milov and H. Satz, Eur. Phys. J. **C66** 377-386 (2010).
- [24] S. Wheaton *et al.*, hep-ph/0407174; S. Wheaton and J. Cleymans, Comput. Phys. Commun. **180**, 84 (2009).
- [25] C. Alt *et al.* (NA49 Collaboration), Eur. Phys. J. **C45**, 343 (2006).
- [26] T. Anticic *et al.* [NA49 Collaboration], Eur. Phys. J. **C68**, 1 (2010).
- [27] T. Anticic *et al.* [NA49 Collaboration], Eur. Phys. J. **C65**, 9 (2010).
- [28] <https://edms.cern.ch/document/1075059/4>
- [29] S. V. Afanasev *et al.* [NA49 Collaboration], Phys. Lett. **B491**, 59 (2000).
- [30] B. I. Abelev *et al.*, Phys Rev. **C79**, 034909 (2009).
- [31] B. I. Abelev *et al.*, Phys Rev. **C75**, 064901 (2007).

- [32] B. I. Abelev *et al.*, Phys Rev. **C79**, 064903 (2009).
- [33] K. Aamodt *et al.*, Eur. Phys. J. **C71**, 1655 (2011).
- [34] K. Aamodt *et al.*, Eur. Phys. J. **C71**, 1594 (2011).
- [35] J. Adam *et al.*, Eur. Phys. J. **C75**, 226 (2015).
- [36] B. I. Abelev *et al.*, Phys. Lett. **B712**, 309 (2012); E. Abbas *et al.*, Eur. Phys. J. **C73**, 2496 (2013).
- [37] B. I. Abelev *et al.*, Eur. Phys. J. **C72**, 2183 (2012).
- [38] J. Cleymans, H Oeschler, K Redlich and S Wheaton, J. Phys. **G32**, 12 (2006).
- [39] A. Andronic, P. Braun-Munzinger and J. Stachel, Nucl. Phys. **A834**, 237c-240c (2010).